

AERODYNAMICS AND SPACE MOTION OF ELASTIC PARACHUTE

Victor Koldaev - koldaev@iae.cta.br

Instituto de Aeronáutica e Espaço, Centro Técnico Aeroespacial, Divisão de Sistemas Espaciais, 12228-904, São José dos Campos, SP, Brasil

Maurício Guimarães da Silva - mgsilva@lcca7.feg.unesp.br

Universidade Estadual de São Paulo, Faculdade de Engenharia de Guaratinguetá, Av. Agenor Pires da Fonseca, 129, 12500000, Guaratinguetá, SP, Brasil.

Abstract. *The process of design of parachute recovery system for sub-orbital or orbital platforms includes a numerical technique application to predict the flow-fields around parachute and aeroelastic effects during space motion of system. This work presents mathematical description and numerical solution of parachute interaction with medium during its unsteady space motion along trajectory with the help of equations of ballistics, aerodynamics, material elasticity and canopy form-shaping. Presented solution takes into consideration the aerodynamic analysis with the 3D-flow simulation over the surface of canopy. The emphasis of the solver aerodynamic is on multiblock. Within each block, the governing equations were discretized using the Beam Warming implicit approximate factorization algorithm. The implicit Euler method is adopted for the time march and second order accurate central difference formulas are used to approximate the spatial derivatives that appear in the governing equations. The proposed method makes it possible to simulate the aeroelastic parachutes functioning. The example illustrates its wide latitude.*

Keywords: *System ballistics, Parachute elasticity, Aerodynamic analysis.*

1. INTRODUCTION

Future space exploration exhibits specifications for return of materials processed in space and quick access to the samples by users, which can best be accomplished by recoverable capsules. The present work discusses the applied numerical method for a recovery system to be used for small orbital platforms based on parachutes. The process of design of recovery system for such capsules needs development of numerical techniques to predict unsteady fluid flow fields around parachute, aeroelastic effects, canopy-capsule stability, opening shock and snatch load during deployment and motion of system in resting medium.

There are a lot of good numerical methods widespread in Computational Fluid Dynamics (CFD) of parachutes. Their direct application to aeroelastic problem of flexible shell is complicated because of high element displacement, strains and unsteady interaction with fluid. The finite-element method (FEM) is used in recent work, (Sahu *et al.*, 1995) to study the 3D aeroelastic ribbon and cross canopies in static solution.

The discrete vortex method (DVM) with the help of FEM is used by Rysev *et al.* (1996) to solve the unsteady parachute aeroelasticity problem. The ellipsoid-cone-shape canopy inflation of penetrable axisymmetric parachute has been presented by Goman *et al.* (1993). In recent works the solution of aerodynamic equations is described and form-shaping equations are solved under fixed differential. After determination and fixation of new form of surface and its element velocities, the pressure differential is determined at new temporal layer. It is

clear that during the temporal step the results for pressure differential and so on for unsteady motion of light membrane can change much.

The Large Particles Method (LPM) was coupled with DVM by Rysev *et al.* (1996) to simulate the 3D dynamics of aeroelastic surfaces. LPM is a very fast method for unsteady 3D simulation of compressible flow with ability to run computations for movable grid fitting to canopy motion. But LPM is not applicable for low subsonic speed because the time decrement is proportional to the dimensionless cell fluid velocity. Another Arbitrary Lagrangian-Eulerian (ALE) method was presented by Aganin *et al.* (1987) for study of parachute inflation. ALE method can be used for simulation of dynamics in 3D flow with large range of speed. In all applications of FEM the mesh generation for arbitrary 3D shell made of fabric is difficult. So, there are a lot of methods for parachute aerodynamics simulation, but no one can be selected as the best.

The subject of the present work is the development of user-friendly applied numerical method for aeroelastic problem with an integration of structural, aerodynamic and flight parachute dynamics problems.

2. BALLISTICS OF THE SYSTEM

Motion of the parachute-capsule system is considered in the reference system, which is in the relatively immovable resting medium. It is considered that motion of parachute system takes place along trajectory of small curvature, when its radius R , Figure 1, is much larger than parachute system dimensions.

Having assumed that parachute axis of symmetry is always directed along capsule velocity vector, parachute system motion can be considered as if it is completely determined by capsule motion. Capsule will be considered as a material body, which have a mass m_c , velocity $V_s(t)$ and a known drag area $C_c S_c$. In consequence of this assumption, capsule motion will take place under the influence of the its weight ($m_c g$), the sum of suspension lines tensions $T(t)$ and the aerodynamic drag. Let us introduce the rectangular coordinate system XOY , Figure 1, having directed OX axis along capsule velocity vector. Then, the equations of system motion on the axis of the coupled coordinate system OX and OY can be written

$$m_c a_x(t) = - m_c g \sin\theta(t) - T(t) - C_c S_c \rho V_s^2/2 \quad (1)$$

$$m_c a_y(t) = m_c V_s^2(t)/R(t) = - m_c g \cos\theta(t) \quad (2)$$

where a_x axial acceleration of capsule, m/s^2
 a_y lateral acceleration of capsule, m/s^2
 g gravity acceleration, m/s^2
 θ flight path angle
 C_c capsule drag coefficient
 S characteristic area of capsule, m^2
 ρ air density, kg/m^3 .

Then, taking $R(t) = V_s(t) d\theta(t)$, the ballistic equations will determine the changes of system trajectory parameters

$$dV_s/dt = - g \sin\theta(t) - [T(t) - C_c S_c \rho V_s^2/2]/m_c \quad (3)$$

$$d\theta/dt = - g \cos\theta(t)/V_s(t) \quad (4)$$

3. FORM SHAPING OF ELASTIC PARACHUTE

The form shaping equations are axisymmetrical, meanwhile the equations of ballistics determine curving of trajectory and, therefore, spoil axis-symmetry of flow. Yet, if curving of motion trajectory of parachute system is insignificant, it can be assumed that axis of symmetry of parachute is all the time directed along the velocity vector of capsule. In this case equations in axisymmetrical form can be used for parachute functioning description.

Form shaping equation of axis-symmetrical parachute can be written in XOY coupled reference system (Figure 2).

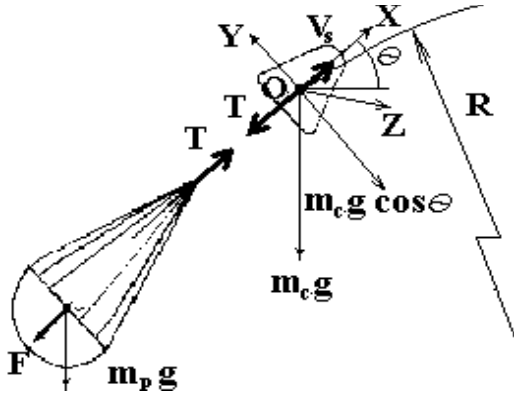


Figure 1 - Modeling of system ballistics

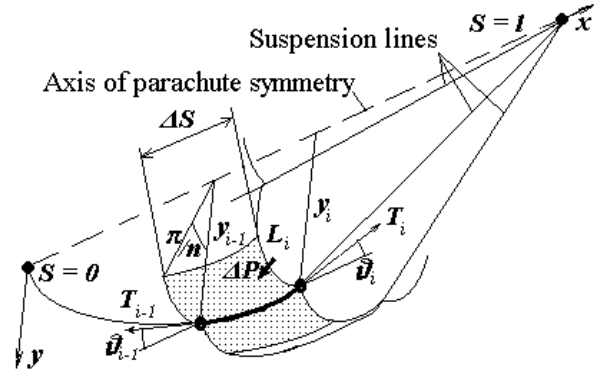


Figure 2 - Canopy form shaping

In consequence of axial symmetry, the equations of suspension line motion under elasticity force effect, aerodynamic forces, effecting through canopy fabric and gravitational force component, effecting along parachute axis of symmetry, are used as equations, which were mentioned above. For parachute with a large quantity of suspension lines $N_{sl} > 16$, the form shaping equations for line element ($L \partial S$) motion along axis OX and OY will have the form

$$\partial S (\gamma_s + \zeta w_f L) \partial^2 x / \partial t^2 = (\gamma_s + \zeta w_f L) g \sin \theta + \partial (T \cos \vartheta) + 2 \partial S \zeta y \sin (\pi / N_{sl}) \Delta P \sin \vartheta \quad (5)$$

$$\partial S (\gamma_s + \zeta w_f L) \partial^2 y / \partial t^2 = \partial (T \sin \vartheta) + 2 \partial S \zeta y \sin (\pi / N_{sl}) \Delta P \cos \vartheta \quad (6)$$

$$\sin \vartheta = \partial y / \partial S \quad (7)$$

$$T = T_{max} (\partial S / \partial S_o - 1) / \varepsilon \quad \text{if} \quad \partial S > \partial S_o \quad (8)$$

$$T = 0 \quad \text{if} \quad \partial S < \partial S_o \quad (9)$$

where γ_s specific mass of suspension line, kg/m

ζ control parameter of line ($\zeta = 0$ where fabric is absent, $\zeta = 1/2$ at point where fabric bears from one side of line and $\zeta = 1$ at point where fabric bears against two sides)

w_s specific mass of fabric, bearing against suspension line, kg/m²

L size of canopy gore, m

S running coordinate along suspension line

S_o running coordinate along suspension line in non-stretched condition, m

ΔP canopy pressure differential, Pa

N_{sl} quantity of suspension lines

- T_{max} strength of suspension lines, N
- ε maximum relative deformation
- ϑ angle of suspension line from parachute symmetry axis.

Having taken $S = 0$ at canopy pole and $S = 1$ at thimble point, one can write the initial conditions as $x(0,S) = x(S)$, $y(0,S) = y(S)$, $\partial x(0,S)/\partial t = V_x(t)$, $\partial y(0,S)/\partial t = V_y(t)$, and the boundary conditions as $\partial x(t,0) = 0$, $\partial y(t,0) = 0$, $y(t,1) = 0$ and

$$m_c/N_{sl} \partial^2 y_{x=1} / \partial t^2 = m_c g \sin\theta / N_{sl} - T_s(t,1) \cos\vartheta(t,1) \quad (10)$$

The boundary conditions at thimble have the concentrated factor in the form of payload mass m_p , hence, it is the equation of system motion axially OX under gravity and suspension lines tension. It should be noticed that the last equation in the boundary conditions coincides with the equation (3).

So, having the second equation and the initial conditions of ballistics to form shaping equations together with initial and boundary conditions, it is possible to obtain the complete system of equations describing motion and deformation of axisymmetrical parachute with capsule within set pressure differential at canopy. Discrete analogue of the form shaping equations, mentioned above, can be obtained, using the method of finite elements. Substituting differentials by finite differences and concentrating suspension lines elements masses m_i at the points, distancing one from another for distance ΔS , suspension line aerodynamic equations can be written in the form

$$a_{xi} = -g \sin\vartheta_i + [2\Delta P_i y_i \Delta S_i \zeta_i \sin\vartheta_i \sin(\pi/N_{sl}) + T_i \cos\vartheta_i - T_{i-1} \cos\vartheta_{i-1}] / [\Delta S_i (\gamma_s + \zeta w_f L_i(S))] \quad (11)$$

$$a_{yi} = [2\Delta P_i \Delta S_i \zeta_i \cos\vartheta_i y_i \sin(\pi/N_{sl}) + T_i \sin\vartheta_i - T_{i-1} \sin\vartheta_{i-1}] / [\Delta S_i (\gamma_s + \zeta w_f L_i(S))] \quad (12)$$

Using the initial and boundary conditions, it is possible to determine velocities and displacement of all points of suspension line at time moment Δt_y after the formulas

$$V_{zi}(\Delta t_y) = V_{zi}(0) + a_{zi} \Delta P(\Delta t_y) \Delta t_y \quad (13)$$

$$z_i(\Delta t_y) = \{x_i; y_i\} = z_i(0) + V_z(0) \Delta t_{ym} + a_{zi} \Delta P(\Delta t_y) \Delta^2 t_y / 2 \quad (14)$$

The quantity of the step Δt_y is selected taking into consideration the solution stability according to Currant condition

$$\Delta t_y = \alpha_k \Delta S_p (g \gamma_{sl} \varepsilon / T_{max})^{1/2}, \quad 0 < \alpha_k < 1 \quad (15)$$

Having differential function $\Delta P(S, t)$, it is possible to calculate analogously the motion of suspension line at the time moment $2\Delta t_y, 3\Delta t_y, \dots, k \Delta t_y$ and so on, and moreover

$$V_{sl}(k\Delta t_y) = V_{sl}((k-1)\Delta t_y) + a_{sl} \Delta P(\Delta t_y) \Delta t_y \quad (16)$$

$$z_l(k\Delta t_y) = z_l((k-1)\Delta t_y) + V_{sl}((k-1)\Delta t_y) \Delta t_y + a_{sl} (\Delta P(k \Delta t_y)) \Delta^2 t_y / 2 \quad (17)$$

Pressure differential function $\Delta P(S, t)$ at each time moment is determined within simultaneous solution of aerodynamic equations and suspension line motion equation, the algorithm of which is given below.

4. FORMULATION OF THE AERODYNAMICS PROBLEM

When some of the fluid domain boundaries undergo a motion with large amplitude, it becomes necessary to solve the flow equations on a moving and possibly deforming grid. In the paper, we consider the realistic situation where the fluid and structure problems have different resolution requirements and their computational domains have matching discrete interfaces. Each of the two components of the coupled fluid/structure problem has different mathematical and numerical properties, and distinct software implementation requirements.

The flow solver, used here, has been documented extensively in literature, for example, Sankar et al. (1989), Kwon et al. (1992) e Mello (1994). This solver integrates in time the 3D compressible Euler equations on a curvilinear body-fitted coordinate system (ξ, η, ζ, τ) . If inertial cartesian velocity components are retained as dependent variables, the three-dimensional, unsteady, Euler equations can be transformed to the arbitrary curvilinear space, while retaining strong conservation law form. The resulting transformed equations are not more complicated than the original cartesian set, and can be written

$$\frac{\partial Q}{\partial \tau} + \frac{\partial E}{\partial \xi} + \frac{\partial F}{\partial \eta} + \frac{\partial G}{\partial \zeta} = 0, \quad (18)$$

where Q vector of conserved variables
 E, F and G flux vectors.

A suitable nondimensionalization of the governing equations is assumed in order to write "Eq. (18)". In the present case, the choice of reference state proposed in Pulliam & Steger (1980) is adopted. The cartesian velocity components u, v and w are nondimensionalized with respect to a_∞ (the free-stream speed of sound), density ρ is referenced to ρ_∞ and total energy to $\rho_\infty a_\infty^2$, where ρ_∞ is the air density of standard atmosphere.

The vector of conserved variables defined

$$Q = J^{-1} \{ \rho \quad \rho u \quad \rho v \quad \rho w \quad e \}^T \quad (19)$$

where u, v and w are cartesian velocity components.

Pressure is defined

$$p = (\gamma - 1) \rho e_i = (\gamma - 1) \left[e - \frac{1}{2} \rho (u^2 + v^2 + w^2) \right] \quad (20)$$

where γ is the ratio of specific heats.

Expressions for the required metric terms and for the Jacobian of the coordinate transformation can be found in Pulliam & Steger (1980), among other references.

Due to the complexity of the geometry in the parachute regions, and with the objective of keeping the codes as modular as possible, the decision was made to the implementing multiblock techniques. Within each block, the governing equations were discretized using the Beam Warming implicit approximate factorization algorithm, Mello (1994). The implicit Euler method is adopted for the time march and second order accurate central difference formulas are used to approximate the spatial derivatives that appear in the governing equations as well as the metrics of transformation that link the physical domain $(x, y, z$ and $t)$ with the transformed domain (ξ, η, ζ, τ) . A set of 2nd /4th order non-linear, spectral radius based, explicit artificial dissipation terms are added to the discretized equations. The second

order implicit dissipation is used to help the overall numerical stability of the scheme. When these approximations are used, a system of nonlinear algebraic equations result for the flow properties at a number of points in the flow domain. As it is common with the Newton's method for solving nonlinear equations, these equations are linearized about their values at a previous time level. The matrix of the resulting system of equations contain 5x5 matrix elements, but may be shown to be sparse, banded, and diagonally dominant. This matrix may be approximately factored into two or more tri-diagonal matrices, that may be easily inverted. This matrix may be approximately factored into two or more tri-diagonal matrices, that may be easily inverted. In some instances, using a strategy proposed by Pulliam and Chausse (1981), these factored matrices may be reduced to scalar tridiagonal matrices prior to their inversion. The accuracy and stability characteristics of this baseline methodology are now well understood. The basics ideas underlying the present multiblock algorithm were that each block should be able to internally identify the types of boundaries on its six faces and that each face should consist of one single type of boundary. In the context, the solution procedure within each block should be implemented in a completely independent fashion. Additional details of a given configuration could be added to the simulation simply by creating new grid blocks that would describe such features. The treatment of block interfaces amounts to an explicit enforcement of boundary conditions across the blocks. The use of multiblock grids is reported in literature with Azevedo (1997), Strauss (1997) among others.

The meshes used in the present work were all generated by algebraic methods within each block. The multisurface algebraic grid generation technique described by Fletcher (1988), has been implemented in a fairly general code for the present configuration.

Figure 3 shows the numbers and sizes of the three-dimensional cylindrical grid for parachute canopy, which are suggested in the present work.

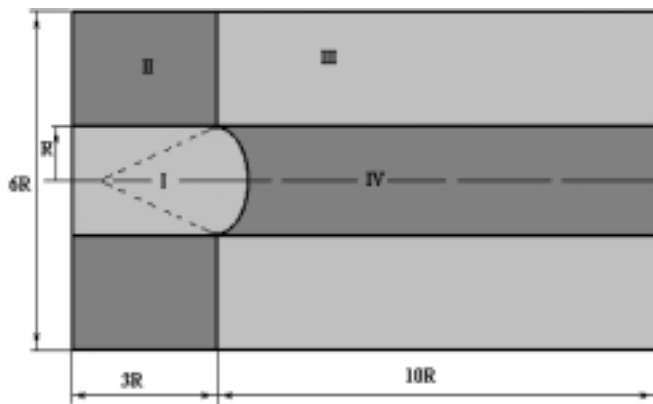


Figure 3 – Blocks sizes of the cylindrical grid

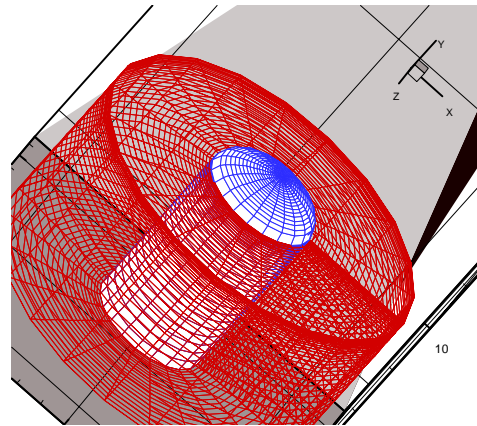


Figure 4 – Sells of first and second blocks

The code allows for grid clustering at various regions along the radial and axial directions (Figure 4).

Hyperbolic tangent grid stretching function is used in order to obtain the desired grid clustering and coarsening over the body. It is important to realize that since the goal is to perform aeroelastic analyses, the body will be deforming as the solution proceeds. This means that some form of grid reshaping is necessary in order to account for this deformation. In the present approach, the complete grid in each block is regenerated at every time step, which is another reason why it is important to use algebraic grid generation methods which are very fast (Azevedo, 1988).

5. SOME RESULTS OF SIMULATION

The aerodynamics of the axisymmetrical parachute has been simulated for initial Mach number $M = 0.5$ and canopy surface radius $R = 3$ m. Figure 5 shows the unsteady flow around the non-permeable opened parachute at the moment when the wake vortex is separating from the canopy.

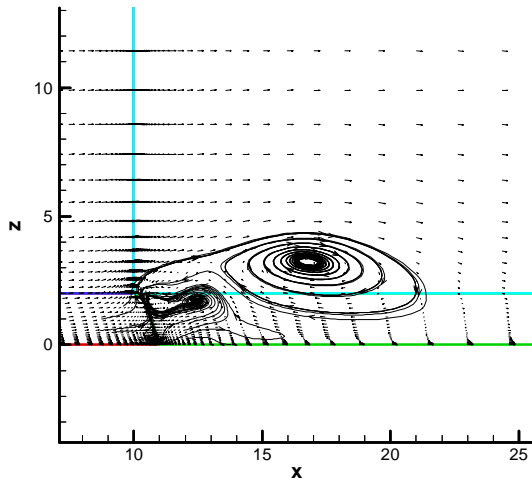


Figure 5 – Simulation of unsteady flow streams around canopy (the sizes are in m)

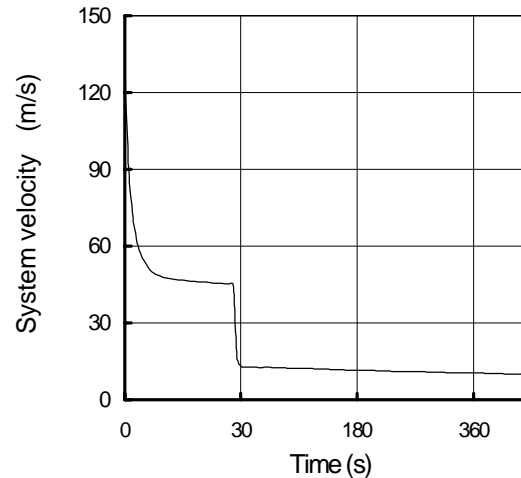


Figure 6 – Flight dynamics simulation of the parachute system

Analysis of flow formation around opened canopy shows that its relative symmetry remains only soon after the beginning of flow development. Within this, lateral components of wake flow velocity along canopy axis of symmetry at the first phase are close to zero. With the flow development, a part of wake cord-vortex is repulsed backwards and in some moment it separates from canopy (Figure 5). The zone of separation constantly displaces along the canopy edge, generating a lateral aerodynamic force that changes in direction. At the following phase at each point of aerodynamic trail the spacing periodical components of the flow velocity take place behind the canopy surface. This explains rotation and oscillation of non-penetrable canopy in airflow, including the case of its absolute symmetry. Therefore, it is necessary to consider the 3D airflow for all canopy configurations. In the case of penetrable canopy simulation due to use of canopy windows or cloth porosity, the canopy movement stability significantly increases because of the reduction of wake vortex intensity.

The parachute flight dynamics during the system motion on trajectory has been simulated with payload mass of $m_c = 215$ kg, initial angle of trajectory $\theta = -90^\circ$, drag parachute area 4 m² and main parachute area 27 m². At an altitude of 6 km with the initial velocity of 135 m/s, after the container door separation, the drag parachute canopy is filled under the influence of the air stream flow. In the process the capsule decelerates down to the speed of 45 m/s (Figure 6). At 4500-m altitude the device releases the deployment bags and opens the main parachutes. Then, the drag parachute canopy ejects deployment bags off from the main parachutes and due to the connection of the drag parachute canopy with the main parachutes points of junction, keeps them from filling too quickly, decreasing the main parachutes opening force. In the process of the capsule descending by the main parachutes the rate of descent of the system decreases to 10 m/s.

6. CONCLUSIONS

The unsteady problem solution of parachute system motion in space has been elaborated. The proposed method makes it possible to simulate the 3D flow around parachute, calculate aeroelastic process of inflation and flight dynamics of parachute system on the trajectory. The axisymmetrical canopy aerodynamics and system motion simulations are presented for recoverable capsule.

Acknowledgements

The first author would like to express his gratitude to CNPq for supporting him as visiting scientist (Grant No. 300.186/96-7) at the Space Systems Division of the Aeronáutica e Espaço, Centro Técnico Aeroespacial.

REFERENCES

- Aganin, A, Gilmanov, F., Kuznetsov, V., 1987, The Simulation of Shell-Fluid Interaction Based on ALE Method and Conservative Interpolation, J. Shell-Fluid Flow Interaction, Academy of Science of the USSR, Kazan.
- Azevedo, J. L. F., 1988, Transonic Aeroelastic Analysis of Launch Vehicle Configurations, NASA CR-4186.
- Azevedo, J. L. F., Strauss, D., e Ferrari, M.A.S., 1997, Viscous Multiblock Simulations of Axisymmetric Launch Vehicle Flows, AIAA Paper 97-2300, Proceedings of the 15th AIAA Applied Aerodynamics Conference, Part 2, AIAA CP-78, Atlanta, GA, p.664.
- Goman, O., Karpluk, V., Nisht, M., Sudakov, A., 1993, Numerical Simulation of Axisimmetrical Separated Flow of Incompressible Fluid, Mashinostroenie, Moscow.
- Koldaev, V., Guimaraes, M. and Moraes, P., 1999, Simulation of Parachute Dynamics, XV Brazilian Congress of Mechanical Engineering, COBEM, Aguas de Lindoia.
- Kwon, O.J. and Sankar, L.N., 1992, Viscous Flow Simulation of Fighter Aircraft, J. of Aircraft, Vol. 29, No. 5, pp886-891.
- Mosseev, Y., 1997, The Multipurpose Integrated Software for Structural and Aeroelastic Analysis of Decelerators, Paragliders and Balloons, 14th AIAA Aerodynamic and Decelerator Systems Technology Conference, AIAA 97-1455, San Francisco.
- Macha, J., 1993, A Simple Approximate Model of Parachute Inflation, AIAA Paper 93-1206..
- Mello, A. O. F., 1994, Improved Hybrid Navier Stokes/Full Potential Method for Computation of Unsteady Compressible Viscous Flows, Tese de Doutorado, Atlanta.
- Pulliam, T. and Chaussee, D., 1981, A Diagonal Form of Implicit Appoximate Factorization Algorithm, J. Computational Physics, Vol. 39, pp. 347-363.
- Pulliam, T. H., and Steger, J. L., 1980, Implicit Finite-Difference Simulations of Three-Dimensional Compressible Flow, AIAA Journal, Vol. 18, No. 2, pp.159-167.
- Rysev, O., Ponomarev, A., Vasiliev, M., Vishniak, A., Dneprov, I., Mosseev, Y., 1996, Parachute Systems. "Nauka" publ. Company, Russian Academy of Science, Moscow.
- Sankar, L. N. and Kwon, O. J., 1989, High Alpha Simulation of Fighter Aircraft, NASA CP-3149, pp 689-702
- Sahu, J., Cooper, G., Benney, R., 1995, 3D Parachute Descent Analysis Using Coupled CFD and Structural Codes, 13-th AIAA Aerodynamic Decelerator Systems Technology Conference, AIAA 95-1558.
- Strickland, J. & Higuchi, H., 1996, Parachute Aerodynamics: An Assessment of Prediction Capability. Journal of Aircraft, Vol.33, N^o2.
- Fletcher, C. A. J., 1988, Computational Techniques for Fluid Dynamics 2. Specific Techniques for Different Flow Categories, Springer-Verlag, Berlim (Chapt. 13).